

**JPET #222281**

**Title:** The Novel Anticancer Drug Hydroxytriolein Inhibits Lung Cancer Cell Proliferation Via a PKC $\alpha$  and ERK1/2 Dependent Mechanism.

**Authors:** Francisca Guardiola-Serrano, Roberto Beteta-Göbel, Raquel Rodríguez-Lorca, Maitane Ibarguren, David J. López, Silvia Terés, Rafael Alvarez, María Alonso-Sande, Xavier Busquets & Pablo V. Escribá.

**JPET #222281**

**Running title:** Hydroxytrirolein Inhibits Lung Cancer Cell Proliferation.

**Corresponding author:** Francisca Guardiola-Serrano, Laboratory of Molecular Cell Biomedicine, Department of Biology, University of the Balearic Islands, E-07122 Palma, Balearic Islands, Spain. E-mail: [franciscaguardiola@uib.es](mailto:franciscaguardiola@uib.es). Phone: +34971173331. Fax:+34971173184.

**Abbreviations:** Baf. A1, bafilomycin A1; DAG, diacylglycerol; DAGK, diacylglycerol kinase; DCFH-DA, 2',7'-dichlorofluorescein diacetate; ERK, extracellular signal-regulated kinase; FFA, free fatty acids; GF, GF109203X, 2-[1-(3-Dimethylaminopropyl)-1H-indol-3-yl]-3-(1H-indol-3-yl)maleimide, Bisindolylmaleimide I; HTO, hydroxytrirolein; MAPK, mitogen-activated protein kinase; MEK, mitogen-activated protein/extracellular signal-regulated kinase kinase; NAC, N-acetylcysteine; NSCLC, non-small-cell lung cancer; LPL, lipoprotein lipase; OA, oleic acid; PMS, N-methyl dibenzopyrazine methyl sulfate; POPE, 1-palmitoyl-2-oleoyl-sn-glycero-3-phosphoethanolamine; PKC $\alpha$ , protein kinase C alpha; ROS, reactive oxygen species; TG, triacylglycerides; Vit.E,  $\alpha$ -tocoferol; XTT, sodium 3'-[1-(phenylaminocarbonyl)-3,4-tetrazolium]-bis (4 methoxy-6-nitro)benzene sulfonic acid hydrate) 5-dimethylthiazol-2-yl]-2, 5- diphenyltetrazoliumbromide.

Number of tables: 1, number of figures: 8, number of references: 55, number of text pages: 32.

Word count introduction: 630.

Word count discussion: 1500.

Word count abstract: 244.

Supplementary data: 3 tables, 4 figures and supplementary methods.

**Section assignment:** Drug discovery and translational medicine.

## JPET #222281

### Abstract

Membrane lipid therapy is a novel approach to rationally design or discover therapeutic molecules that target membrane lipids. This strategy has been used to design synthetic fatty acid analogues that are currently under study in clinical trials for the treatment of cancer. In this context, and with the aim of controlling tumor cell growth, we have designed and synthesized a hydroxylated analogue of triolein, hydroxytriolein (HTO). Both triolein and HTO regulate the biophysical properties of model membranes and they inhibit the growth of non-small lung cancer cell lines *in vitro*. The molecular mechanism underlying the anti-proliferative effect of HTO involves regulation of the lipid membrane structure, PKC $\alpha$  and ERK activation, the production of reactive oxygen species (ROS) and autophagy. *In vivo* studies on a mouse model of non-small cell lung cancer showed that HTO but not triolein impairs tumor growth, which could be associated with the relative resistance of HTO to enzymatic degradation. The data presented explain in part why olive oil (whose main component is the triacylglyceride triolein) is preventive but not therapeutic, and they demonstrate a potent effect of HTO against cancer. HTO shows a good safety profile, it can be administered orally, and it does not induce non-tumor cell (fibroblast) death *in vitro* or side effects in mice, reflecting its specificity for cancer cells. For these reasons, HTO is a good candidate as a drug to combat cancer that acts by regulating lipid structure and function in the cancer cell membrane.

## JPET #222281

### Introduction

Non-small cell lung cancer (NSCLC) accounts for about 80% of all lung cancers and it is one of the leading causes of cancer deaths (Reck et al., 2013). The hypothesis that proliferation in cancer depends on the activity of oncogenic pathways has served to focus the design and discovery of anti-cancer drugs targeted against specific proteins (Lynch et al., 2004; Paez et al., 2004). However, lung cancer has a high 5 year mortality rate due to drug resistance and other problems (Sharma et al., 2007), highlighting an unmet clinical need and the fact that innovative approaches are required to develop new therapies against this devastating condition. We previously defined a new therapeutic approach called membrane-lipid therapy, whereby drugs interact with membrane lipids rather than proteins or nucleic acids (Escriba, 2006). Membrane-lipid therapy targets cell membranes, regulating their structure, the activity of relevant signaling proteins that associate with them and their downstream events (Escriba et al., 2008). Drugs acting on the membrane are both efficacious and specific, in part because they regulate upstream events that affect several proteins. Despite the relatively recent description of this concept (Escriba, 2006), there are already two molecules, whose mechanism of action is based on regulating membrane composition and structure, that have shown safety and efficacy against cancer in clinical trials (*clinicaltrial.gov* identifiers: NCT01792310 and NCT02201823, respectively) (Martin et al., 2013; Ibarguren et al., 2014).

Lipids play several roles in the cell, serving as a source of energy and a supply of building blocks for membrane biosynthesis but also, acting as signaling molecules. Moreover, membrane lipid composition may reflect different stages of a cell and indeed lipid synthesis and localization is actively regulated by cells during cytokinesis (Atilla-Gokcumen et al., 2014). In this context it has been shown that the lipid composition of cancer cells differs from that of their normal counterparts (Meng et al., 2004).

## JPET #222281

There is now considerable evidence that the membrane lipid composition can be modified through diet. The protective effect of the Mediterranean diet against the development of cancer is well known and more specifically, high olive oil consumption is associated with a lower incidence of lung cancer (Fortes et al., 2003), breast cancer and colon cancer (Stark and Madar, 2002). The main constituent of extra virgin olive oil is the triacylglycerol triolein, which contains three oleic acid molecules (OA, 70-80% in olive oil). *In vitro* studies have shown that OA possesses antitumor activity that depends on the type of cancer and it is linked to the inhibition of angiogenesis (Lamy et al., 2013), metastasis (Suzuki et al., 1997) and proliferation (Hughes-Fulford et al., 2001), as well as the induction of apoptosis (Menendez et al., 2005). OA has a protective effect against chemically induced lung tumorigenesis (Yamaki et al., 2002) and it inhibits metastasis of Lewis Lung Carcinoma (LLC), although it has no significant effect on the primary solid tumor (Kimura, 2002).

The antitumor potential of triolein is limited due to its use as a cell fuel. Triolein is degraded by lipoprotein lipases (LPL) and the fatty acids released are used to provide energy via  $\beta$ -oxidation. We designed HTO as a more stable triolein analogue (Fig. 1A) that is metabolized by LPL at a markedly lower rate than triolein. Moreover, the resulting hydroxyoleate molecule cannot be degraded by  $\beta$ -oxidation but by  $\alpha$ -oxidation which is a slower catabolic pathway. Because both synthetic lipids (the hydroxylated triacylglyceride and the hydroxylated fatty acid) have antitumor activity, their efficacy is in part due to their enhanced metabolic stability.

In this study, we have used several human NSCLC lines as a model to evaluate the antitumor potential of HTO and its natural analogue from olive oil, triolein. Accordingly, we found that substitution of 3 hydrogen atoms by hydroxyl moieties increased the antitumorigenic and therapeutic potential of triolein.

## JPET #222281

### Methods

**Reagents and Antibodies.** 1-palmitoyl-2-oleoyl-sn-glycero-3-phosphoethanolamine (POPE) was purchased from Avanti Polar Lipids Inc. (Alabaster, Alabama). 1,2 diolein was from Larodan (Malmö, Sweden). HTO was obtained from Lipopharma (Palma de Mallorca, Spain). Triolein, oleic acid, rhodamine B and the fluorescent probe 2'7'-dichlorofluorescein diacetate (DCFH-DA) were purchased from Sigma-Aldrich (St. Louis, MO). The PKC inhibitor GF109203X (2-[1-(3-Dimethylaminopropyl)-1H-indol-3-yl]-3-(1H-indol-3-yl)maleimide, Bisindolylmaleimide I) was obtained from Tocris (Bristol, United Kingdom), the MEK inhibitor U0126 (1,4-Diamino-2,3-dicyano-1,4-bis[2-aminophenylthio]butadiene) from Promega (Madison, WI) and bafilomycin A1 from Sigma-Aldrich (St. Louis, MO). The antibodies used for Western blotting were raised against: LC3BI-II, MAP kinase kinase (MEK), phospho-MEK (p-MEK), extracellular signal-regulated kinase (anti-ERK), phospho-ERK (p-ERK: all purchased from Cell Signaling, Danvers, MA). The antibody against gelsolin was purchased from BD transduction laboratories (New Jersey, USA) and the anti- $\alpha$  tubulin from Sigma-Aldrich (St. Louis MO).

**Differential Scanning Calorimetry.** DSC measurements were made on a TA 2920 calorimeter (TA Instruments, New Castle, Delaware, USA). Briefly, 15 mg of POPE was mixed with 1 mol% of HTO or triolein, all compounds previously dissolved in chloroform:methanol (2:1, v:v). The lipid mixtures were dried under argon flux and solvent traces were removed under vacuum for at least 3 h at room temperature prior to hydration. Multilamellar lipid vesicles were formed by resuspending the lipid film in 10 mM HEPES, 100 mM KCl, 1 mM EDTA [pH 7.4], following eight freeze/thaw cycles (-196 °C / 40 °C). The mixture was loaded into aluminium, hermetic pans, and it was subjected to five consecutive scans between -10 and 80 °C at a scan rate of 1 °C/min. The transition enthalpy and transition temperature values shown here correspond to

## JPET #222281

the means of all the measured scans and they were obtained using the manufacturer's software (TA Universal Analysis).

**Average Lipid Droplet Size.** The HTO emulsion was centrifuged at 116,000 x g for 1 h 30 min and the resulting pellet was stained with 1% of phosphotungstic acid (Sigma-Aldrich, St. Louis, MO) for 1 min, allowed to dry on an electron microscope grid, and the droplet size was determined on a Hitachi H-600 Kv50 transmission electron microscope. The size of the HTO aggregates was also measured by dynamic light scattering on a Brookhaven 90 Plus instrument. HTO emulsion was prepared as indicated and the light scattered of 659 nm was detected at 90° at room temperature.

**Cell Lines and Culture.** Human non-small cell lung cancer cells (A549, Calu-1, HOP-62, NCI-H838) and normal lung fibroblasts (MRC-5) were obtained from the American Type Culture Collection (Manassas, VA). The cells were incubated at 37 °C in a humidified atmosphere of 5% CO<sub>2</sub> in RPMI 1640 (A549, Calu-1, HOP-62, NCI-H838) or DMEM (MRC-5) medium supplemented with 10% fetal bovine serum (FBS, v/v), 100 units/mL penicillin and 0.1 µg/mL streptomycin. MRC-5 medium was also supplemented with 1% of non-essential amino acids. Media and non-essential amino acids were obtained from Sigma-Aldrich (St Louis, MO), penicillin-streptomycin from Biowest (Nuaillé, France) and FBS from Biosera (Boussens, France).

**HTO Incorporation into Cells.** HTO emulsion containing 1 mM Rhodamine B was stirred for 24 h and then sonicated for 2 min. Cells were seeded at a density of  $5 \times 10^4$  cells/well in 6-well plates and on the following day, they were treated with the HTO emulsion containing rhodamine B. The cells were then fixed with 4% paraformaldehyde and their nucleus was stained with Hoechst 33342 (Thermo-scientific, Waltham, Ma) before visualizing them on a Nikon Eclipse TG 2000-S fluorescence microscope.

**Cell Proliferation Assays.** Cell number was measured by trypan blue exclusion, whereby the cells were stained with trypan blue and the viable cells were counted in a

## JPET #222281

Burker chamber. Metabolically active cells were measured using the cell proliferation kit II from Roche. Briefly, cells were cultured in 96-well plates at a density of  $3 \times 10^3$  cells per well, in the presence or absence of HTO or triolein and at the concentrations indicated in the figures. After different periods the viable cells in the plate were measured, mixing XTT (sodium 3'-[1-(phenylaminocarbonyl)-3,4-tetrazolium]-bis (4-methoxy-6-nitro) benzene sulfonic acid hydrate) 5-dimethylthiazol-2-yl]-2, 5-diphenyltetrazoliumbromide) with PMS (N-methyl dibenzopyrazine methyl sulfate) and adding it to the cell culture medium according to manufacturer's recommendations (Roche, Basel, Switzerland). The cells were incubated at 37 °C and in 5% CO<sub>2</sub> until the color developed and absorbance was determined at 495 nm using a microplate reader with a reference wavelength of 650 nm (FLUOstar Omega, BMG LABTECH, Germany).

**Lactate Dehydrogenase Release.** Lactate dehydrogenase (LDH) release from cells after drug treatment was measured with the cytotoxicity detection kit<sup>PLUS</sup> (LDH from Roche, Basel, Switzerland) according to manufacturer's recommendations. Briefly cells were cultured in 96-well plates at a density of  $3 \times 10^3$  cells per well, in the presence or absence of HTO and at the concentrations indicated in the figures. After 24 h, 2.5% lysis buffer was added to some cells to assess the maximum release of LDH. Next, cell culture medium was collected, LDH reagent was added to the medium and incubated at room temperature at dark until color developed, absorbance was determined at 492 nm using a microplate reader (FLUOstar Omega, BMG LABTECH, Germany). Test medium was used as a background control. Cytotoxicity was analyzed compared to control cells using the following equation:  $((\text{HTO treated}-\text{untreated})/(\text{maximum LDH}-\text{untreated})) \times 100$ .

**LPL Activity.** LPL activity was determined by measuring the levels of glycerol using a kit to test the triacylglyceride concentration according to the manufacturer's instructions (Biosystems, Barcelona, Spain). For this purpose, triolein or HTO were



## JPET #222281

dissolved in ether (8 mM), which was evaporated under N<sub>2</sub> atmosphere, and the triacylglyceride concentration of the samples was measured. Briefly, 1 ml of reagent containing lipase and the other products to test the appearance of glycerol was mixed together and the absorbance at 500 nm was measured after 20 min or 1 h on a microplate reader (FLUOstar Omega, BMG LABTECH, Germany).

**Electrophoresis, Immunoblotting and Protein Quantification.** Cells were cultured in 10 cm<sup>2</sup> culture plates at a density  $3.5 \times 10^5$  cells per well. After incubating in the presence or absence of HTO at the concentrations and times indicated in the figure, 300  $\mu$ l of protein extraction buffer was added to each plate: 10 mM Tris-HCl [pH 7.4], 50 mM NaCl, 1 mM MgCl<sub>2</sub>, 2 mM EDTA, 1% SDS, 5 mM iodoacetamide and 1 mM PMSF. The cell suspensions were disrupted by ultrasound (70% cycle) for 10 s at 50 w using a Braun Labsonic U (probe-type) sonicator, and 30  $\mu$ l aliquots were removed for protein quantification using a modified Lowry assay according to the manufacturer's instructions (Bio-Rad, California, USA). Subsequently, 30  $\mu$ l of 10x electrophoresis loading buffer (120 mM Tris-HCl [pH 6.8], 4% SDS, 50% glycerol, 0.1% bromophenol blue and 10%  $\beta$ -mercaptoethanol) was added and the samples were boiled for 5 min. For immunoblotting, 30-50  $\mu$ g of total protein from the cell lysates was resolved by SDS polyacrylamide gel electrophoresis (SDS-PAGE) and transferred to nitrocellulose membranes (Schleicher & Schüell). The membranes were then blocked for 1 h at room temperature in PBS containing 5% non-fat dry milk and 0.1% Tween 20 (blocking solution), and they were then incubated overnight at 4 °C with a primary antibody diluted in blocking solution. The membranes were then washed three times for 5 min with PBS and the antibody was detected with a donkey anti-mouse or donkey anti-rabbit IgG labeled with IRDye®800CW (1:5000). Proteins were quantified by image analysis of the membranes scanned at 800 nm using the infrared imaging system Odyssey (Li-COR, Nebraska, USA). The  $\alpha$ -tubulin content in the samples was

## **JPET #222281**

determined by the same procedure and used as a loading control. The intensity of the signal was analyzed using the program Total Lab (Nonlinear Dynamics Ltd).

**Generation of Reactive Oxygen Species (ROS).** A549 cells were seeded in 6 cm<sup>2</sup> plates at a density of  $1 \times 10^5$  cells/plate and cultured at 37 °C in the presence or absence of HTO for 24 h or 48 h in 5% CO<sub>2</sub>, as described above. The cells were then harvested, washed with PBS and resuspended in 300 µl of 10 µM 2',7'-dichlorofluorescein diacetate for 30 min at 37 °C. Samples were then analyzed immediately on a flow cytometer EPICS XL-MCL (Beckman Coulter, Mi, FL) with 488 nm excitation wavelength.

**Lipid Separation.** A549 cells were seeded in 10 cm<sup>2</sup> culture plates at a density of  $4 \times 10^5$  cells/plate and cultured in the presence or absence of HTO for 24 h. Membrane lipids were extracted directly from a monolayer of ca.  $1 \times 10^6$  cells by chloroform:methanol extraction (Bligh and Dyer, 1959). Protein levels were measured using a modified Lowry assay according to the manufacturer's instructions (Bio-Rad, California, USA). Individual neutral lipids classes were separated by TLC on Whatman silica gel-60 plates (20 × 20 cm) using petroleum ether/diethylether/acetic acid (75:25:1.3 by volume). After TLC separation, the plates were air-dried, sprayed with 8% (wt/vol) H<sub>3</sub>PO<sub>4</sub> containing 10% (wt/vol) CuSO<sub>4</sub>, and charred at 180 °C for 10 min before the lipids were quantified by photodensitometry. The lipid fractions were identified using 1,2 diolein, oleic acid and triolein as standards.

**Cell Fractionation.** A549 cells were seeded in 25 cm<sup>2</sup> culture plates at a density of  $2 \times 10^6$  cells/plate in the presence or absence of HTO. Approximately,  $4 \times 10^6$  cells were used for cell fractionation, first homogenizing the cells with a 25G needle in 600 µl of lysis buffer (20 mM HEPES, 2 mM EDTA, 0.5 mM EGTA, 1.5 mM MgCl<sub>2</sub>, 1 mM cantaridine, 1 mM ortovanadate and a protein inhibitor cocktail from Roche) and then by ultrasound (10% cycle for 20 s at 50 w using a Braun Labsonic U probe). The cell

## JPET #222281

lysates were centrifuged at 1,000 x g for 10 min at 4 °C and the supernatant was ultracentrifuged at 90,000 x g for 1 h at 4 °C. The membrane pellets were suspended in the same volume as the cytosolic fraction (supernatant), in lysis buffer containing 1% SDS. The same volume of the fractions was loaded onto the gels.

**Animals, Tumor Xenografts and Treatments.** NUDE (Swiss) Crl:NU (Ico)-Foxn1<sup>nu</sup> mice (five-week-old, 30–35 g, Charles River Laboratories, Paris, France) were maintained in a thermostated cabinet with a sterile air flow (28 °C, EHRET, Labor-U-Pharmatechnik) at a relative humidity of 40–60%, on a 12 h dark/light cycle and with autoclaved food and water supplied *ad libitum*. To induce subcutaneous xenograft tumors,  $7.5 \times 10^6$  non-small A549 cells were inoculated into the dorsal area on one side of the animal and after one week the tumors were visible. Animals were then randomly divided into groups with a similar mean tumor volume, and for 29 days they received daily p.o. treatment with HTO or triolein (400 mg/kg), or the vehicle alone (water). Tumor volumes ( $v$ ) were calculated as  $v = W^2 \times L / 2$  where  $w$  is the tumor width and  $L$  its length. All experiments were carried out in accordance with the animal welfare guidelines of the European Union and the Institutional Committee for Animal Research of the University of the Balearic Islands.

**Data Analysis.** Statistical analyses were performed using GraphPad Prism 4.01 (GraphPad Software Inc., San Diego, CA). Unless otherwise indicated, the data are expressed as the mean  $\pm$  SEM of at least three independent experiments with duplicate samples. Experimental groups were compared using one-way ANOVA followed by the Bonferroni's multiple-comparison test or a Student's  $t$  test. The differences between experimental groups were considered statistically significant at  $p < 0.05$ : \* $p < 0.05$ , \*\* $p < 0.01$ , and \*\*\* $p < 0.001$ .

## JPET #222281

### Results

**Triolein and HTO Regulate Membrane Lipid Structure.** We studied the effect of triolein and HTO on membrane lipid structure using differential scanning microcalorimetry and small angle X-ray diffraction. Microcalorimetry showed no differences in the gel-to-fluid ( $L\beta$ -to- $L\alpha$ ) transition temperature of 1-palmitoyl-2-oleoyl-sn-glycero-3-phosphoethanolamine (POPE) model membranes in the presence or absence of either hydroxylated or non-hydroxylated triacylglyceride. By contrast, a drop in the lamellar-to-inverted hexagonal ( $L\alpha$ -to- $H_{II}$ ) phase transition temperature ( $T_H$ ) was observed in the presence of 1 mol% triolein or HTO (from 69 °C to ca. 61 °C and ca. 66 °C, respectively: Table 1). Moreover, the presence of 5 mol% HTO dramatically reduced the  $T_H$ , and it increased the temperature range in which the  $L\alpha$  and  $H_{II}$  phases coexist, which is associated with a reduction in the bilayer's lateral surface pressure (from ca. 24 °C: Supplemental Fig. 1). This property of the bilayer influences the type and abundance of peripheral membrane proteins bound to the membrane.

**HTO Impairs the Proliferation and Viability of Human Non-Small Cell Lung Cancer Cell lines.** To treat cells in culture we formulated HTO as a lipid emulsion in which the average droplet size was ca. 0.3  $\mu$ m, with small polydispersity when measured with the nanosizer (Supplemental Table 1, Supplemental Fig. 2A). The HTO in this emulsion clearly entered the cells, as witnessed when the emulsion was loaded with rhodamine, this marker was readily detected in the A549 cells by fluorescence microscopy (Fig. 1B).

When the proliferation of NSCLC cells was evaluated, exposure to HTO reduced the number of viable cells in a dose- and time-dependent manner (Fig. 2A-C). Cells showed standard growth dynamics in the absence of HTO, while exposure to 150-300  $\mu$ M HTO induced NSCLC cell death (Fig. 2D and Supplemental Fig. 2B). To determine whether the drop in the number of viable A549 cells was due to cell death or to cell

## JPET #222281

cycle arrest, we examined the extent of apoptosis by flow cytometry of propidium iodide (PI) and annexin V labeled cells. In this context, the presence of HTO significantly increased the number of early and late apoptotic cells, concomitant with a decrease in the number of viable cells (Supplemental Fig. 2C).

The cytotoxicity of HTO was also analyzed in non-tumor fibroblast (MRC-5) cells and the IC<sub>50</sub> value proved to be higher than that for A549 cells (>500 μM and 36.3 μM: Fig. 2E), which reflects the lack of signs of HTO toxicity observed in animals (see below). These results further suggest that HTO acts specifically against tumors.

Triolein and HTO provoked a reduction in NSCLC cell number at all studied times, short incubation times (24 h) showed no significant difference between HTO and triolein IC<sub>50</sub> (Fig. 2C). After 72 h, the IC<sub>50</sub> values obtained for HTO and triolein in A549 (32 ±3.9 μM vs 60.85 ±8.5 μM) and NCI-H838 (49.8 ±16.7 μM vs 301.5 ±61.6) were significantly different (p<0,05). Moreover in NCI-H838 the difference in the IC<sub>50</sub> values was already significant (p<0,01) after 48 h (117.74 ±15.4 μM vs 401.9 ±55.2 μM).

**Differential LPL Degradation of Triolein and HTO.** When we measured LPL activity *in vitro*, HTO degradation was 4-fold slower for HTO than that for triolein (Fig. 2F), which indicates that the metabolism of HTO *in vivo* could be impaired by the hydroxyl groups presence in the acyl moieties.

**HTO Activates the MAP Kinase (ERK) Pathway.** Sphingomyelin levels increased significantly in the membranes of cells exposed to HTO (300 μM) for 48 h (Supplemental Fig. 2D-E). Changes in membrane lipid composition of tumor cells have been related to altered cell signaling that might impair tumor growth (Pardini, 2006). We analyzed the phosphorylation status (i.e., activity) of the MAP kinase pathway signaling proteins ERK and MEK in human A549 cells, and we found a significant increase in phosphorylated ERK and MEK after a 24 h and 48 h exposure to HTO (Fig. 3A and Supplemental Fig. 3A-B). Increases in ERK phosphorylation (activation) were

## **JPET #222281**

significant in NCI-H838 cells, but did not reach statistical significance in Calu-1 and HOP-62 cells (Fig. 3B-C).

**HTO Induces ROS Production.** ROS mediated signaling has been associated with sustained ERK activation (Cagnol and Chambard, 2010) and a 24 or 48 h exposure to HTO increased ROS levels in a dose-dependent manner (Fig. 3D). To investigate how ROS production influences the activity of HTO against cancer, we evaluated the effects of HTO on A549 cells in the presence or absence of the ROS scavengers,  $\alpha$ -tocopherol (vitamin E) or N-acetylcysteine. Of these,  $\alpha$ -tocopherol alone abolished the increase in ROS levels induced by HTO (Fig. 3E) and blocked the HTO-induced death of A549 cells (Fig. 3F). In addition to its antioxidant activity,  $\alpha$ -tocopherol activates the diacylglycerol kinase (DAGK) that induces the conversion of diacylglycerol to phosphatidic acid (Lee et al., 1999). DAG increases significantly in cells exposed to HTO (Fig. 4C), activating PKC $\alpha$ , such that this kinase may be inhibited by  $\alpha$ -tocopherol. To confirm whether PKC $\alpha$  is involved in the antitumor mechanism of HTO, we investigated the cytosolic-to-membrane translocation of this enzyme. HTO impaired PKC $\alpha$  translocation to cytosol and PKC $\alpha$  clearly accumulated in the membrane fraction of HTO treated cells, which is associated with its enzymatic activation (Fig. 4A-B).

**The Antiproliferative Effects of HTO and triolein are Mediated by PKC $\alpha$ .** To determine whether PKC $\alpha$  was involved in the inhibition of A549 cell growth provoked by HTO, A549 cells were exposed to HTO or triolein in the presence or absence of general or specific PKC inhibitors. The antiproliferative effect of both triolein and HTO was reverted in the presence of  $\alpha$ -tocopherol (Vit.E) or the PKC inhibitor GF109203X (GF), further demonstrating the involvement of PKC in effect of HTO against tumors (Fig. 5A). Because PKC $\alpha$  activation is associated with cancer cell differentiation, we analyzed gelsolin as a marker of differentiation. Both HTO and triolein enhanced the

## **JPET #222281**

levels of gelsolin protein, an increase that was impeded by  $\alpha$ -tocopherol and GF (Fig. 5B-C).

**ERK Activation through PKC is Responsible for the Effect of HTO on A549 Cell Growth.** ERK phosphorylation (i.e.: activation) increased markedly and significantly in the presence of HTO and to a lesser extent in the presence of triolein (Fig. 5B-D). By contrast, ERK was not activated in the presence of the PKC inhibitors GF or  $\alpha$ -tocopherol, indicating that PKC was responsible for the rise in ERK phosphorylation. ERK is directly phosphorylated by MEK and indeed, HTO and triolein failed to inhibit A549 cell growth in the presence of the MEK inhibitor, U0126 (Fig. 5E). General or specific PKC and MEK inhibitors reverted the HTO cytotoxicity in all studied cell lines, although they only reverted HTO-antiproliferative effect in Calu-1 cells (Fig. 5 F-G).

**HTO Induces Autophagy.** Autophagy serves as a pathway of recycling intracellular components, it occurs at a some basal level in all cells and increases in response to multiple stressors such as ROS accumulation and PKC alpha activation (Kroemer et al., 2010; Sridharan et al., 2011). Moreover, it has been reported that excessive levels of autophagy can induce a form of cell death called autophagic cell death (Liu and Levine, 2015). To investigate the effect of HTO on autophagy, we analyzed the levels of the autophagy marker LC3B-II. Upon induction of autophagy, LC3B-I is converted to LC3B-II by an ubiquitin-like conjugation system which conjugates a phosphatidylethanolamine (PE) moiety to LC3B-I. LC3B-II is more hydrophobic than LC3B-I and therefore migrates more rapidly in SDS-PAGE compared to LC3B-I. HTO induced a marked increase in LC3B-II levels in all studied cell lines (Fig. 6 A-C). Higher levels of LC3-II could be associated either with enhanced autophagosome synthesis or reduced autophagosome turnover. To distinguish between these two options we treated the cells with bafilomycin A1, a known inhibitor of the late phase of autophagy which acts by inhibiting vacuolar H<sup>+</sup>-ATPase thereby inhibiting lysosome acidification and increasing the levels of LC3B-I/II. Our results showed that bafilomycin A1

## **JPET #222281**

increased the levels of the autophagy marker LC3B-II both in control and HTO treated cells (Fig. 6D), which indicates efficient autophagic signal propagation in HTO treated cells.

### **HTO Inhibits Tumor Progression in a Xenograft Model of Human Lung Cancer.**

The Irwin test was performed in NUDE (Swiss) Crl:NU (Ico)-Foxn1nu mice and no abnormalities were detected in the animal behavior at concentrations as high as 1500 mg/kg (Supplemental Table 2 and Supplemental Table 3). The efficacy of HTO and triolein against NSCL was tested in an A549 cell xenograft model of human lung cancer. HTO treatment (400 mg/Kg per day) induced a marked and significant reduction in A549 tumors, whereas triolein appeared to only modestly reduced the volume of human lung cancer-derived tumors in a manner that failed to reach significance (Fig. 7A). During the treatment, no changes in mice weight (Fig. 7B), mortality or side effects were observed in association with HTO or triolein treatment, indicating that their oral administration was well tolerated. Moreover, sacrifice at the end of the treatment and autopsy to some animals revealed no macroscopic signs of toxicity on the lung, kidney, heart or stomach, no fat accumulation was observed in the liver and normal feces were found in the intestine.



## JPET #222281

### Discussion

We have designed and synthesized a hydroxy-triacylglyceride (HTO) analogous to triolein that shows antitumor activity *in vitro* and that prevents tumor progression *in vivo* (Fig. 8). Lipid intake has been shown to modify the composition of cell membranes, regulating their biophysical properties and influencing protein-membrane interactions, thereby affecting cell signaling, metabolism and viability (Spector and Burns, 1987; Barcelo-Coblijn et al., 2011; Teres et al., 2012). HTO and triolein induce changes in membrane lipid composition and structure that might be associated with their antitumor activity, as shown previously for other anti-cancer drugs (Martinez et al., 2005). The triacylglyceride (TG) content of the cell membrane is lower than that of other lipid species (Lerique et al., 1994). However, exposing cells to HTO and triolein not only increases TG content but also free fatty-acids and diacylglycerol, which in turn increase the non-lamellar ( $H_{II}$ ) phase propensity of membranes (this work and ref. (Ibarguren et al., 2014). An increase in the non-lamellar phase propensity of lipid bilayers causes a reduction in the lateral surface pressure that controls the type and abundance of the signaling proteins that regulate cell proliferation, differentiation and survival (Escriba et al., 1995; Martin et al., 2013).

In this scenario, non-lamellar prone lipids promote the cytoplasmic-to-membrane translocation of PKC (Goldberg et al., 1994; Escriba et al., 1995) and therefore, its activity (Epand et al., 1991; Goldberg and Zidovetzki, 1998). We show here that HTO induces PKC $\alpha$  cytosol to membrane translocation and that PKC $\alpha$  is in part responsible for the antitumor effects of HTO. Through the stimulation of the protein phosphatase, PP2A,  $\alpha$ -Tocopherol specifically inactivates PKC $\alpha$  and in turn, it dephosphorylates PKC $\alpha$  (Ricciarelli et al., 1998) and blocks HTO-induced cell death. PKC $\alpha$  activation has been formerly related to cell proliferation and also, to differentiation. Due to its effects on proliferation, PKC inhibition has been considered as a potential cancer therapy. However, PKC $\alpha$  levels are low in NSCLC cells and it was recently demonstrated that

## JPET #222281

PKC $\alpha$  functions as a tumor suppressor in the *LSL-Kras in vivo* murine lung-adenocarcinoma model. In these mice the loss of PKC $\alpha$  leads to self-renewal and proliferation of broncho-alveolar stem-cells. In lung cells, PKC $\alpha$  activates p38, regulating TGF $\beta$  signaling, which may be oncogenic in the presence of K-Ras (Hill et al., 2014). In addition, PKC $\alpha$  has been seen to negatively regulate the Wnt/ $\beta$ -catenin signaling, which is upregulated in some cancers like NSCLC (Stewart, 2014). Most NSCLC cell lines have active Wnt signaling and in the A549 cell-line, activation of the Wnt pathway has been associated to cisplatin resistance (Gao et al., 2013). Active PKC $\alpha$  phosphorylates  $\beta$ -catenin, inducing degradation of this proliferation-promoting protein through the proteasome system. Indeed, antisense oligonucleotides against PKC $\alpha$  were not efficient in a phase-III trial in patients with NSCLC (Paz-Ares et al., 2006). Our results with HTO suggest that the activation of PKC $\alpha$  could be beneficial for NSCLC treatment, although further studies will be necessary to determine to what extent HTO can affect the TGF $\beta$  and Wnt/ $\beta$ -catenin signaling pathways.

We found that HTO activation of PKC $\alpha$  promoted, on the one hand, sustained ERK activation and ROS production and on the other, increased levels of the actin-binding protein and cell-differentiation marker gelsolin. The correlation between gelsolin expression and tumorigenesis is controversial. Reduced gelsolin expression appears to be characteristic of a variety of transformed cells (Mullauer et al., 1993), yet high gelsolin levels are associated with poor survival in some sub-populations of NSCLC patients (Yang et al., 2004). This effect is possibly due to the fact that gelsolin may facilitate tumor dissemination and metastasis by promoting locomotion. However, there is a loss of gelsolin protein in late-stage NSCLCs and it is weakly expressed or undetectable in most NSCLC-cell-lines (Dosaka-Akita et al., 1998). Gelsolin protein levels increase when lung cancer cells receive differentiation stimuli (Jarrard et al., 1998) and we previously detected cancer (glioma) cell differentiation after membrane

## JPET #222281

lipid remodeling as an intermediate step prior to programmed cell death (Teres et al., 2012).

Fatty acids can induce ROS production through mitochondrial events (Schonfeld and Wojtczak, 2008) and by enhanced activity of the NAD(P)H-oxidase stimulated by PKC (Chen et al., 2014). ROS are known to produce apoptosis and to act as mediators in signal transduction pathways, like the mitogen-activated-protein (MAP) kinase pathway (Cagnol and Chambard, 2010). HTO triggered ERK activation and its role in the antitumor effects of HTO was evident by the recovery of A549-cell growth upon inhibition of ERK phosphorylation. Nevertheless, the effects of sustained ERK activation depends on the cell type, and it varies from cell cycle arrest in hepatoma cells (HepG2) (Wen-Sheng, 2006) to apoptosis in leukemia cells (Stadheim and Kucera, 1998). In this context, exposing A549-cells to HTO and the ROS scavenger N-acetylcysteine does not inhibit cell death, indicating that the main stimulus activating ERK is PKC. Thus, PKC $\alpha$  phosphorylation of the Raf-kinase-inhibitory protein, RKIP-1, will impair Raf inhibition and therefore trigger ERK activation (Corbit et al., 2003).

To investigate the potential toxicity of HTO and triolein, we measured their effects on the growth of tumor (NSCLC-cells) and non-tumor (MRC-5 fibroblast) cells. Thus, HTO and triolein impair the growth of NSCLC cells but not that of normal-lung fibroblasts. These differences could in part be attributed to the fact that HTO can rapidly alter the membrane composition of cancer cells, given the high turnover of the tumor cell phospholipid fraction (Spector and Burns, 1987). HTO induces rapid and marked changes in the levels of membrane phospholipids, including an ca. two-fold increase in the sphingomyelin:phosphatidylethanolamine ratio (Supplemental Fig. 2E). These changes have been associated with the translocation of inactive peripheral membrane proteins to the cytosol (e.g., Ras) and the loss of proliferation potential (Teres et al., 2012). Accordingly, PKC phosphorylates K-Ras in A549-cells, promoting its translocation from the plasma membrane to intracellular membranes within the cell,

## JPET #222281

including those of the mitochondria (Bivona et al., 2006). The translocation of mutated active K-Ras from the plasma membrane to the cytoplasm reduces its oncogenic potential. Moreover, active K-Ras interacts with mitochondrial mBcl-X<sub>L</sub> and can induce apoptosis.

One reason to design triolein analogues was to augment the activity of olive oil (i.e.: triolein) against cancer, introducing radicals that would impair their metabolism. We measured HTO and triolein metabolism by LPL and we found that the latter was degraded ca. 4-fold faster than HTO *in vitro*. In addition, increased LPL activity has been reported in cancer tumors compared to normal-lung tissue, most likely due to the energy requirements of tumor cells (Cerne et al., 2007), potentially explaining the lack of efficacy of olive oil despite its protective anticancer effects. LPL would hydrolyze triacylglycerides to fatty acids that the tumor could use as energy source. Indeed, higher LPL activity is inversely correlated with NSCLC patient survival (Trost et al., 2009). Further studies will be necessary to clarify whether the activity of this enzyme is inhibited by the presence of HTO or if its activity is low due to lower affinity for HTO.

HTO induced an autophagy response in all studied cell lines which origins could be traced to the known inducers of the autophagy response: increase in ROS, ERK or PKC $\alpha$  activation (Kroemer et al., 2010; Sridharan et al., 2011). Moreover, HTO treatment induce lipid droplets (data not shown), a major depot of neutral lipids such as triglycerides, which, have been reported to increase autophagy (Dupont et al., 2014). Oleate has recently been reported to trigger a non-canonical autophagy response which relies on an intact Golgi apparatus (Niso-Santano et al., 2015). Given the similarity between HTO and triolein (both containing fatty-acyl-moieties hydroxtioleate and oleate respectively), we hypothesized that HTO induced autophagy would also depend on an intact Golgi apparatus.

## JPET #222281

In summary, HTO has a stronger anti-tumorigenic effect than triolein, the major triacylglyceride of olive oil. Epidemiological studies have shown that olive oil markedly prevents the occurrence of several types of cancer but that it lacks therapeutic activity (Martin-Moreno; Stark and Madar, 2002; Fortes et al., 2003). Moreover, OA-rich oils have protective effects against tumor growth and metastasis in animal models (Kimura, 2002; Yamaki et al., 2002). Consistent with these studies, our data indicate that triolein, and most likely OA, could have protective effects against tumorigenesis but no therapeutic activity against lung cancer. By contrast, hydroxylated triolein (HTO) displays a high efficacy against NSCLC both *in vitro* and *in vivo*. Both triolein and HTO induce similar changes in membrane structure and they have similar effects *in vitro*. The differences observed *in vivo* might be due to the lower rate of HTO metabolism, as described for OA and its hydroxylated analogue (Llado et al., 2010). In addition, HTO processing by LPL yields hydroxylated OA that, in contrast to OA, increases sphingomyelin synthase activity. The result is an increase in membrane sphingomyelin levels, which has been associated with the induction of cancer cell arrest, differentiation and death (Barcelo-Coblijn et al., 2011; Teres et al., 2012; Martin et al., 2013). Indeed, increased sphingomyelin synthase expression and gene copy number have been associated with longer cancer patient survival. Therefore, HTO constitute a new anticancer drug class with great potential.

## Acknowledgements

The authors thank Dr. Daniel López for his help with LPL activity assays.

## **JPET #222281**

### **Authorship Contributions**

The authors have made the following declarations about their contribution: anticancer drug design and synthesis: Escribá. Experimental design: Escribá, Guardiola-Serrano. Acquisition, analysis and interpretation of data: Guardiola-Serrano, Beteta-Göbel, Rodríguez-Lorca, Ibarguren, López, Terés, Álvarez, Alonso-Sande. Writing and/or revision of manuscript: Guardiola-Serrano, Escribá, Busquets. Financing: Escribá, Busquets.

## JPET #222281

### References

- Atilla-Gokcumen GE, Muro E, Relat-Goberna J, Sasse S, Bedigian A, Coughlin ML, Garcia-Manyes S and Eggert US (2014) Dividing cells regulate their lipid composition and localization. *Cell* **156**:428-439.
- Barcelo-Coblijn G, Martin ML, de Almeida RF, Noguera-Salva MA, Marcilla-Etxenike A, Guardiola-Serrano F, Luth A, Kleuser B, Halver JE and Escriba PV (2011) Sphingomyelin and sphingomyelin synthase (SMS) in the malignant transformation of glioma cells and in 2-hydroxyoleic acid therapy. *Proc Natl Acad Sci U S A* **108**:19569-19574.
- Bivona TG, Quatela SE, Bodemann BO, Ahearn IM, Soskis MJ, Mor A, Miura J, Wiener HH, Wright L, Saba SG, Yim D, Fein A, Perez de Castro I, Li C, Thompson CB, Cox AD and Philips MR (2006) PKC regulates a farnesyl-electrostatic switch on K-Ras that promotes its association with Bcl-XL on mitochondria and induces apoptosis. *Mol Cell* **21**:481-493.
- Bligh EG and Dyer WJ (1959) A rapid method of total lipid extraction and purification. *Can J Biochem Physiol* **37**:911-917.
- Cagnol S and Chambard JC (2010) ERK and cell death: mechanisms of ERK-induced cell death--apoptosis, autophagy and senescence. *Febs J* **277**:2-21.
- Cerne D, Melkic E, Trost Z, Sok M and Marc J (2007) Lipoprotein lipase activity and gene expression in lung cancer and in adjacent noncancer lung tissue. *Exp Lung Res* **33**:217-225.
- Corbit KC, Trakul N, Eves EM, Diaz B, Marshall M and Rosner MR (2003) Activation of Raf-1 signaling by protein kinase C through a mechanism involving Raf kinase inhibitory protein. *J Biol Chem* **278**:13061-13068.
- Chen F, Yu Y, Haigh S, Johnson J, Lucas R, Stepp DW and Fulton DJ (2014) Regulation of NADPH oxidase 5 by protein kinase C isoforms. *PLoS One* **9**.

**JPET #222281**

- Dosaka-Akita H, Hommura F, Fujita H, Kinoshita I, Nishi M, Morikawa T, Katoh H, Kawakami Y and Kuzumaki N (1998) Frequent loss of gelsolin expression in non-small cell lung cancers of heavy smokers. *Cancer Res* **58**:322-327.
- Dupont N, Chauhan S, Arko-Mensah J, Castillo EF, Masedunskas A, Weigert R, Robenek H, Proikas-Cezanne T and Deretic V (2014) Neutral lipid stores and lipase PNPLA5 contribute to autophagosome biogenesis. *Curr Biol* **24**:609-620.
- Epand RM, Epand RF, Leon BT, Menger FM and Kuo JF (1991) Evidence for the regulation of the activity of protein kinase C through changes in membrane properties. *Biosci Rep* **11**:59-64.
- Escriba PV (2006) Membrane-lipid therapy: a new approach in molecular medicine. *Trends Mol Med* **12**:34-43.
- Escriba PV, Gonzalez-Ros JM, Goni FM, Kinnunen PK, Vigh L, Sanchez-Magraner L, Fernandez AM, Busquets X, Horvath I and Barcelo-Coblijn G (2008) Membranes: a meeting point for lipids, proteins and therapies. *J Cell Mol Med* **12**:829-875.
- Escriba PV, Sastre M and Garcia-Sevilla JA (1995) Disruption of cellular signaling pathways by daunomycin through destabilization of nonlamellar membrane structures. *Proc Natl Acad Sci U S A* **92**:7595-7599.
- Fortes C, Forastiere F, Farchi S, Mallone S, Trequattrinni T, Anatra F, Schmid G and Perucci CA (2003) The protective effect of the Mediterranean diet on lung cancer. *Nutr Cancer* **46**:30-37.
- Gao Y, Liu Z, Zhang X, He J, Pan Y, Hao F, Xie L, Li Q, Qiu X and Wang E (2013) Inhibition of cytoplasmic GSK-3 $\beta$  increases cisplatin resistance through activation of Wnt/ $\beta$ -catenin signaling in A549/DDP cells. *Cancer Letters* **336**:231-239.



**JPET #222281**

- Goldberg EM, Lester DS, Borchardt DB and Zidovetzki R (1994) Effects of diacylglycerols and Ca<sup>2+</sup> on structure of phosphatidylcholine/phosphatidylserine bilayers. *Biophys J* **66**:382-393.
- Goldberg EM and Zidovetzki R (1998) Synergistic effects of diacylglycerols and fatty acids on membrane structure and protein kinase C activity. *Biochemistry* **37**:5623-5632.
- Hill KS, Erdogan E, Khor A, Walsh MP, Leitges M, Murray NR and Fields AP (2014) Protein kinase Calpha suppresses Kras-mediated lung tumor formation through activation of a p38 MAPK-TGFbeta signaling axis. *Oncogene* **33**:2134-2144.
- Hughes-Fulford M, Chen Y and Tjandrawinata RR (2001) Fatty acid regulates gene expression and growth of human prostate cancer PC-3 cells. *Carcinogenesis* **22**:701-707.
- Ibarguren M, Lopez DJ and Escriba PV (2014) The effect of natural and synthetic fatty acids on membrane structure, microdomain organization, cellular functions and human health. *Biochim Biophys Acta* **3**:00460-00464.
- Jarrard JA, Linnoila RI, Lee H, Steinberg SM, Witschi H and Szabo E (1998) MUC1 is a novel marker for the type II pneumocyte lineage during lung carcinogenesis. *Cancer Res* **58**:5582-5589.
- Kimura Y (2002) Carp oil or oleic acid, but not linoleic acid or linolenic acid, inhibits tumor growth and metastasis in Lewis lung carcinoma-bearing mice. *J Nutr* **132**:2069-2075.
- Kroemer G, Marino G and Levine B (2010) Autophagy and the integrated stress response. *Mol Cell* **40**:280-293.
- Lamy S, Ouanouki A, Beliveau R and Desrosiers RR (2013) Olive oil compounds inhibit vascular endothelial growth factor receptor-2 phosphorylation. *Exp Cell Res* **8**:00515-00516.

**JPET #222281**

- Lee IK, Koya D, Ishi H, Kanoh H and King GL (1999) d-Alpha-tocopherol prevents the hyperglycemia induced activation of diacylglycerol (DAG)-protein kinase C (PKC) pathway in vascular smooth muscle cell by an increase of DAG kinase activity. *Diabetes Res Clin Pract* **45**:183-190.
- Lerique B, Lepetit-Thevenin J, Verine A, Delpero C and Boyer J (1994) Triacylglycerol in biomembranes. *Life Sci* **54**:831-840.
- Liu Y and Levine B (2015) Autosis and autophagic cell death: the dark side of autophagy. *Cell Death Differ* **22**:367-376.
- Lynch TJ, Bell DW, Sordella R, Gurubhagavatula S, Okimoto RA, Brannigan BW, Harris PL, Haserlat SM, Supko JG, Haluska FG, Louis DN, Christiani DC, Settleman J and Haber DA (2004) Activating mutations in the epidermal growth factor receptor underlying responsiveness of non-small-cell lung cancer to gefitinib. *N Engl J Med* **350**:2129-2139.
- Llado V, Gutierrez A, Martinez J, Casas J, Teres S, Higuera M, Galmes A, Saus C, Besalduch J, Busquets X and Escriba PV (2010) Minerval induces apoptosis in Jurkat and other cancer cells. *J Cell Mol Med* **14**:659-670.
- Martin-Moreno JM *The role of olive oil in lowering cancer risk: is this real gold or simply pinchbeck?* *J Epidemiol Community Health*. 2000 Oct;54(10):726-7.
- Martin ML, Barceló-Coblijn G, de Almeida RFM, Noguera-Salvà MA, Terés S, Higuera M, Liebisch G, Schmitz G, Busquets X and Escribá PV (2013) The role of membrane fatty acid remodeling in the antitumor mechanism of action of 2-hydroxyoleic acid. *Biochimica et Biophysica Acta (BBA) - Biomembranes* **1828**:1405-1413.
- Martinez J, Vogler O, Casas J, Barcelo F, Alemany R, Prades J, Nagy T, Baamonde C, Kasprzyk PG, Teres S, Saus C and Escriba PV (2005) Membrane structure modulation, protein kinase C alpha activation, and anticancer activity of minerval. *Mol Pharmacol* **67**:531-540.

**JPET #222281**

- Menendez JA, Vellon L, Colomer R and Lupu R (2005) Oleic acid, the main monounsaturated fatty acid of olive oil, suppresses Her-2/neu (erbB-2) expression and synergistically enhances the growth inhibitory effects of trastuzumab (Herceptin) in breast cancer cells with Her-2/neu oncogene amplification. *Ann Oncol* **16**:359-371.
- Meng X, Riordan NH, Riordan HD, Mikirova N, Jackson J, Gonzalez MJ, Miranda-Massari JR, Mora E and Trinidad Castillo W (2004) Cell membrane fatty acid composition differs between normal and malignant cell lines. *P R Health Sci J* **23**:103-106.
- Mullauer L, Fujita H, Ishizaki A and Kuzumaki N (1993) Tumor-suppressive function of mutated gelsolin in ras-transformed cells. *Oncogene* **8**:2531-2536.
- Niso-Santano M, Malik SA, Pietrocola F, Bravo-San Pedro JM, Marino G, Cianfanelli V, Ben-Younes A, Troncoso R, Markaki M, Sica V, Izzo V, Chaba K, Bauvy C, Dupont N, Kepp O, Rockenfeller P, Wolinski H, Madeo F, Lavandro S, Codogno P, Harper F, Pierron G, Tavernarakis N, Cecconi F, Maiuri MC, Galluzzi L and Kroemer G (2015) Unsaturated fatty acids induce non-canonical autophagy. *Embo J* **34**:1025-1041.
- Paez JG, Janne PA, Lee JC, Tracy S, Greulich H, Gabriel S, Herman P, Kaye FJ, Lindeman N, Boggon TJ, Naoki K, Sasaki H, Fujii Y, Eck MJ, Sellers WR, Johnson BE and Meyerson M (2004) EGFR mutations in lung cancer: correlation with clinical response to gefitinib therapy. *Science* **304**:1497-1500.
- Pardini RS (2006) Nutritional intervention with omega-3 fatty acids enhances tumor response to anti-neoplastic agents. *Chem Biol Interact* **162**:89-105.
- Paz-Ares L, Douillard JY, Koralewski P, Manegold C, Smit EF, Reyes JM, Chang GC, John WJ, Peterson PM, Obasaju CK, Lahn M and Gandara DR (2006) Phase III study of gemcitabine and cisplatin with or without aprinocarsen, a protein

**JPET #222281**

- kinase C-alpha antisense oligonucleotide, in patients with advanced-stage non-small-cell lung cancer. *J Clin Oncol* **24**:1428-1434.
- Reck M, Heigener DF, Mok T, Soria JC and Rabe KF (2013) Management of non-small-cell lung cancer: recent developments. *Lancet* **382**:709-719.
- Ricciarelli R, Tasinato A, Clement S, Ozer NK, Boscoboinik D and Azzi A (1998) alpha-Tocopherol specifically inactivates cellular protein kinase C alpha by changing its phosphorylation state. *Biochem J* **334**:243-249.
- Schonfeld P and Wojtczak L (2008) Fatty acids as modulators of the cellular production of reactive oxygen species. *Free Radic Biol Med* **45**:231-241.
- Sharma SV, Bell DW, Settleman J and Haber DA (2007) Epidermal growth factor receptor mutations in lung cancer. *Nat Rev Cancer* **7**:169-181.
- Spector AA and Burns CP (1987) Biological and therapeutic potential of membrane lipid modification in tumors. *Cancer Res* **47**:4529-4537.
- Sridharan S, Jain K and Basu A (2011) Regulation of autophagy by kinases. *Cancers* **3**:2630-2654.
- Stadheim TA and Kucera GL (1998) Extracellular signal-regulated kinase (ERK) activity is required for TPA-mediated inhibition of drug-induced apoptosis. *Biochem Biophys Res Commun* **245**:266-271.
- Stark AH and Madar Z (2002) Olive oil as a functional food: epidemiology and nutritional approaches. *Nutr Rev* **60**:170-176.
- Stewart DJ (2014) Wnt signaling pathway in non-small cell lung cancer. *J Natl Cancer Inst* **106**:5.
- Suzuki I, Iigo M, Ishikawa C, Kuhara T, Asamoto M, Kunimoto T, Moore MA, Yazawa K, Araki E and Tsuda H (1997) Inhibitory effects of oleic and docosahexaenoic acids on lung metastasis by colon-carcinoma-26 cells are associated with reduced matrix metalloproteinase-2 and -9 activities. *Int J Cancer* **73**:607-612.

**JPET #222281**

- Teres S, Llado V, Higuera M, Barcelo-Coblijn G, Martin ML, Noguera-Salva MA, Marcilla-Etxenike A, Garcia-Verdugo JM, Soriano-Navarro M, Saus C, Gomez-Pinedo U, Busquets X and Escriba PV (2012) 2-Hydroxyoleate, a nontoxic membrane binding anticancer drug, induces glioma cell differentiation and autophagy. *Proc Natl Acad Sci U S A* **109**:8489-8494.
- Trost Z, Sok M, Marc J and Cerne D (2009) Increased lipoprotein lipase activity in non-small cell lung cancer tissue predicts shorter patient survival. *Arch Med Res* **40**:364-368.
- Wen-Sheng W (2006) Protein kinase C alpha trigger Ras and Raf-independent MEK/ERK activation for TPA-induced growth inhibition of human hepatoma cell HepG2. *Cancer Lett* **239**:27-35.
- Yamaki T, Yano T, Satoh H, Endo T, Matsuyama C, Kumagai H, Miyahara M, Sakurai H, Pokorny J, Shin SJ and Hagiwara K (2002) High oleic acid oil suppresses lung tumorigenesis in mice through the modulation of extracellular signal-regulated kinase cascade. *Lipids* **37**:783-788.
- Yang J, Tan D, Asch HL, Swede H, Bepler G, Geradts J and Moysich KB (2004) Prognostic significance of gelsolin expression level and variability in non-small cell lung cancer. *Lung Cancer* **46**:29-42.

## JPET #222281

### Footnotes

Laboratory of Molecular Cell Biomedicine, Department of Biology, University of the Balearic Islands, E-07122 Palma, Balearic Islands, Spain (F.G.-S., R.B.-G., R.R.-L., D.J.L., M.I., S.T., R.A., M.A.-S., X.B. and P.E.

Lipopharma Therapeutics S.L., Palma, Spain (D.J.L., M.I., S.T., R.A., M.A.-S.).

This work was supported by the Ministerio de Economía y Competitividad Grants BIO2010-21132 and BIO2013-49006-C2-1-R, by the Marathon Foundation, and by the AECC from the Balearic Islands. F.G.-S. holds a contract from the “Fundación Científica de la Asociación Española Contra el Cáncer” which was in part paid by an “Acció especial” from the Government of the Balearic Islands. M.I. and D.J.L. were supported by Torres-Quevedo Research Contracts from the Spanish Ministerio de Economía y Competitividad (PTQ-10-04214 & PTQ-09-02-02113).

## JPET #222281

### Figure Legends

Fig. 1. HTO structure and A549 cell internalization. (A) Structural comparison of HTO and triolein. (B) HTO lipid emulsion mixed with rhodamine B. Cells were treated for 2 or 24 h with the emulsion, fixed with paraformaldehyde 4% and the nuclei were stained with Hoechst 333442. Rhodamine B staining appears in red, nuclei in blue.

Fig. 2. Efficacy of HTO against human non-small cell lung cancer (A549) cells. (A) Time- and concentration-dependent inhibition of human non-small cell lung cancer (A549) cell growth by HTO. Cells were counted after a 24, 48 and 72 h exposure to the indicated concentrations of HTO (mean  $\pm$  SEM of 3 independent experiments). (B) Inhibition of NSCLC (Calu-1, HOP-62 and NCI-H838) proliferation after 72 h exposure to 150  $\mu$ M of HTO. Viable cells were counted using trypan blue exclusion method (mean  $\pm$  SEM of 2 independent experiments with duplicate samples). (C) IC<sub>50</sub> of HTO and triolein growth inhibition of NSCLC cells (mean  $\pm$  SEM of 3 independent experiments): \* $p$ <0.05 (Student's *t* test). (D) Concentration dependent inhibition of cell proliferation (mean  $\pm$  SEM of 3 independent experiments) and cytotoxicity of NSCLC (A549, Calu-1, HOP-62 and NCI-H838; mean  $\pm$  SEM of 2 independent experiments performed in triplicate). (E) Effect of HTO on the proliferation of lung cancer (A549) cells and normal lung fibroblasts (MRC-5). Cells were incubated for 48 h in the presence (HTO) or absence (C) of HTO (150  $\mu$ M) and cell number was measured (XTT assay, mean  $\pm$  SEM of 3 independent experiments): \*\*\* $p$ <0.001. (F) *In vitro* assay of LPL activity in the presence of 10 mM HTO or triolein: \*\*\* $p$ <0.001 (Two-way ANOVA followed by Bonferroni's test).

Fig. 3. Effect of HTO on the MAPK pathway and on the levels of reactive oxygen species. (A-B) Effect of HTO on ERK (MAPK) and MEK (MAPKK) phosphorylation. Cells (A549) were treated for 24 or 72 h in the presence or absence of HTO (0-300  $\mu$ M, bars correspond to mean  $\pm$  SEM values of 3 independent experiments). The insets

## JPET #222281

show representative immunoblots. (B-C) Effect of HTO on ERK phosphorylation. Cells were treated for 24h in the presence or absence of 150  $\mu$ M HTO. Representative western blots are shown. Bars correspond to the mean  $\pm$  SEM values of 2 independent experiments with duplicate samples. (D) Time- and concentration-dependent increase of ROS following HTO treatment was measured by flow cytometry. (E-F)  $\alpha$ -Tocopherol (Vit.E) blocks ROS production and cell death. A549 cells were incubated for 24 h in the presence or absence of HTO (150  $\mu$ M) plus  $\alpha$ -tocopherol (100  $\mu$ M, Vit.E) or N-acetylcysteine (5 mM NAC), and the ROS levels (E) and viable cell number (F) was measured by flow cytometry and with the XTT assay respectively: \* $p$ <0.05, \*\* $p$ <0.01, \*\*\* $p$ <0.001 vs control (ANOVA followed by Bonferroni's test).

Fig. 4. Effect of HTO on lipid composition and PKC $\alpha$  translocation to cell membranes. (A-B) PKC $\alpha$  recruitment to A549 cell membranes after 10 s, 1 h and 24 h in the presence or absence of HTO (150  $\mu$ M). Representative immunoblots are shown. C: cytosolic fraction; M: membrane fraction. Na<sup>+</sup>K<sup>+</sup>-ATPase was used as a membrane marker. Bars correspond to the mean  $\pm$  SEM values of 1 (HTO 10 s) -2 independent experiments. \* $p$ <0.05, \*\* $p$ <0.01 (Student's *t* test). (C) A549 Cells were maintained in the presence or absence of HTO (150  $\mu$ M) plus  $\alpha$ -tocopherol (100  $\mu$ M, Vit. E) for 24 h before lipids were extracted and separated by thin layer chromatography to measure the diacylglycerol (DAG), triacylglycerides (TG) and free fatty acids (FFA). Bars correspond to the mean  $\pm$  SEM values from 3 independent experiments: \* $p$ <0.05, \*\* $p$ <0.01 vs control (ANOVA followed by Bonferroni's test).

Fig. 5. PKC $\alpha$  and the molecular mechanism of HTO and triolein activity. A549 cells were pre-incubated in the presence or absence of 100  $\mu$ M  $\alpha$ -tocopherol (Vit.E) or 10  $\mu$ M of the PKC inhibitor GF109203X (PKCi) for 1 h before exposure to 150  $\mu$ M triolein or HTO. (A) Cell number was measured using the XTT assay: \*\*  $p$ <0.01, \*\*\* $p$ <0.001 vs control cells, #  $p$ <0.001 vs HTO or triolein treated cells (Anova followed by Bonferroni's



## JPET #222281

test). (B-D) Effect of vitamin E (Vit.E) and the PKC inhibitor GF109203X (PKCi) on gelsolin expression (panel C) and on ERK phosphorylation (panel D) after exposure to HTO or triolein. \* $p < 0.05$ , \*\*  $p < 0.01$ , \*\*\* $p < 0.001$  vs control cells. (E) A549 cell number (% of control) after 24 h treatment with HTO and triolein following pre-incubation with 10  $\mu\text{M}$  of the MEK inhibitor U0126 for 2 h. Bars correspond to the mean  $\pm$  SEM of 3 independent experiments. \*\*  $p < 0.01$ , \*\*\* $p < 0.001$  vs control untreated cells. (F) Cell proliferation and cytotoxicity of NSCLC (Calu-1, HOP-62 and NCI-H838) following HTO co-treatment with either Vit.E or PKC inhibitor GF109203X (PKCi). Bars correspond to the mean  $\pm$  SEM of 3 independent experiments. Proliferation analysis \* $p < 0.05$ , \*\*  $p < 0.01$ , \*\*\* $p < 0.001$  vs control cells. (G) Cell proliferation and cytotoxicity of HTO following MEK inhibition on NSCLC (Calu-1, HOP-62 and NCI-H838). Cells were pre-incubated with 10  $\mu\text{M}$  of the MEK inhibitor U0126 for 2 h and then incubated for 24 h with HTO (HTO) or left untreated (C). Bars correspond to the mean  $\pm$  SEM of 3 independent experiments. Proliferation analysis \* $p < 0.05$ , \*\* $p < 0.01$ , \*\*\* $p < 0.001$  vs control (ANOVA followed by Bonferroni's test).

Fig. 6. HTO induces autophagy. Effect of HTO on LC3B-I levels and on LCBI-II ratio. NSCLC were treated for 24 h in the presence or absence of HTO. (A) A549 cells were treated with 0-300  $\mu\text{M}$  HTO. Bars correspond to mean  $\pm$  SEM values of 3 independent experiments. Representative immunoblots are shown: \* $p < 0.05$ , \*\* $p < 0.01$ , \*\*\* $p < 0.001$  (ANOVA followed by Bonferroni's test). (B-C) Calu-1, HOP-62 and NCI-H838 were treated for 24 h or 72 h with 150  $\mu\text{M}$  HTO. Bars correspond to the mean  $\pm$  SEM values of 2 independents with duplicate samples: \*\* $p < 0.01$ , \*\*\* $p < 0.001$  (Student t test). (D) Effect of bafilomycin A1 on LC3B-I levels of HTO treated cells. A549, HOP-62 and NCI-H838 were pre-treated with 50 nM bafilomycin A (Baf. A1) for 2 h before exposure to 150  $\mu\text{M}$  of HTO.

## JPET #222281

Fig. 7. HTO and triolein inhibits tumor progression *in vivo*. A549 cells ( $7.5 \times 10^6$ ) were injected subcutaneously into nude mice, which were then treated for 30 days (400 mg/kg daily, p.o.) with triolein or HTO. Tumor size (A) was measured with a digital caliper and tumor volume was expressed relative to the volume at the beginning of the treatment (mean  $\pm$  SEM, n=7 for all experimental groups): \*\*\*p<0.001, \*p<0.05 (Student's *t* test). Mice weight (B) was measured during the treatment; full circles correspond to the control HTO group, empty circles to HTO group, full triangles to the control triolein group and empty triangles to the triolein group. (C) Tumor size of the HTO group (day 20) compared to triolein group (day 34).

Fig. 8. Molecular and cellular effects of HTO on A549 lung cancer cells. The antitumor effects of HTO are in part explained by its effects on the biophysical properties of membranes and by the rise in DAG and sphingomyelin. These membrane lipid alterations induced PKC $\alpha$  translocation to the membrane (i.e., activation), which in turn triggered ERK activation and ROS production, provoking increased autophagy and cell death. HTO augmented lipid droplets in the cells which also increased autophagy. HTO hydrolysis by LPL released 2OH-OA (2OH-FFA) and 2OH-DAG, which also have antitumor effects. DAG, diacylglycerol; ERK, extracellular-signal regulated kinases; FFA, free fatty acids; HTO, hydroxytriolein; LPL, lipoprotein lipase; MEK, mitogen-activated protein/ extracellular signal-regulated kinase kinase; PKC $\alpha$ , protein kinase C alpha; ROS, reactive oxygen species.

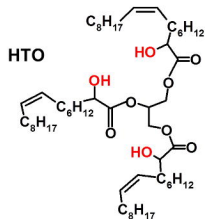
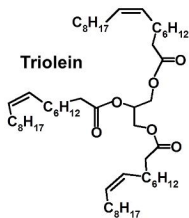
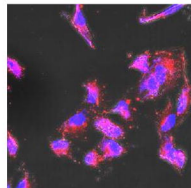
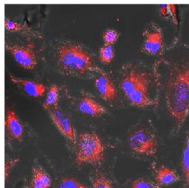
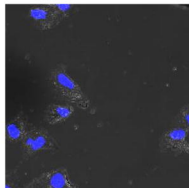
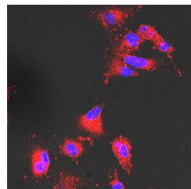
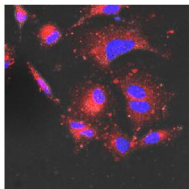
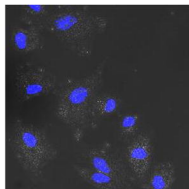
**JPET #222281**

Table 1. HTO and triolein decrease the phase transition temperature of the membrane lamellar-to-hexagonal phase ( $H_{II}$ ). Differential scanning microcalorimetry was carried out on POPE membranes in the presence or absence of 1% of HTO or triolein:  $T_m$  = gel-to-liquid crystalline (lamellar) phase transition temperature;  $T_H$  = lamellar-to-hexagonal ( $H_{II}$ ) phase transition temperature;  $\Delta H$  = transition enthalpy.

POPE vs triolein or HTO: \* $p < 0.01$ , \*\* $p < 0.001$ .

**Lamellar-to-hexagonal phase ( $H_{II}$ ) transition temperature**

Model membrane	$T_m$ (°C)	$\Delta H$ (Kcal/mol)	$T_H$ (°C)	$\Delta H$ (Kcal/mol)
POPE	23.6±0.2	4.42±0.03	69.1±0.5	0.42±0.03
+ Triolein	23.3±0.2	4.55±0.09 <sup>*</sup>	60.8±3.3 <sup>**</sup>	0.24±0.11 <sup>**</sup>
+ HTO	23.8±0.3	5.78±0.08 <sup>**</sup>	66.0±0.9 <sup>*</sup>	0.55±0.06 <sup>**</sup>

**A****B****[HTO]****0 $\mu$ M****150 $\mu$ M****300 $\mu$ M****2h****24h****Fig. 1**

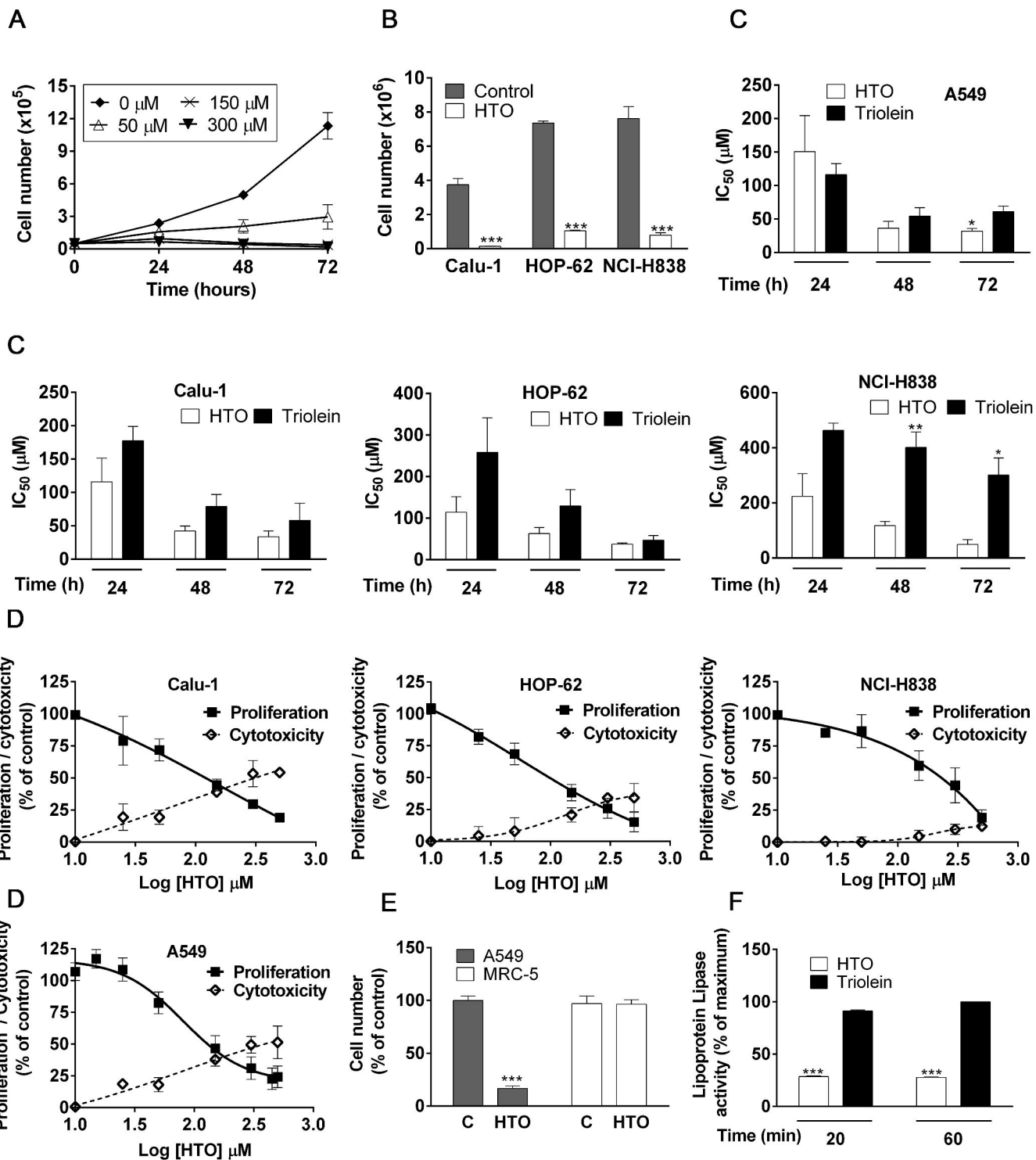
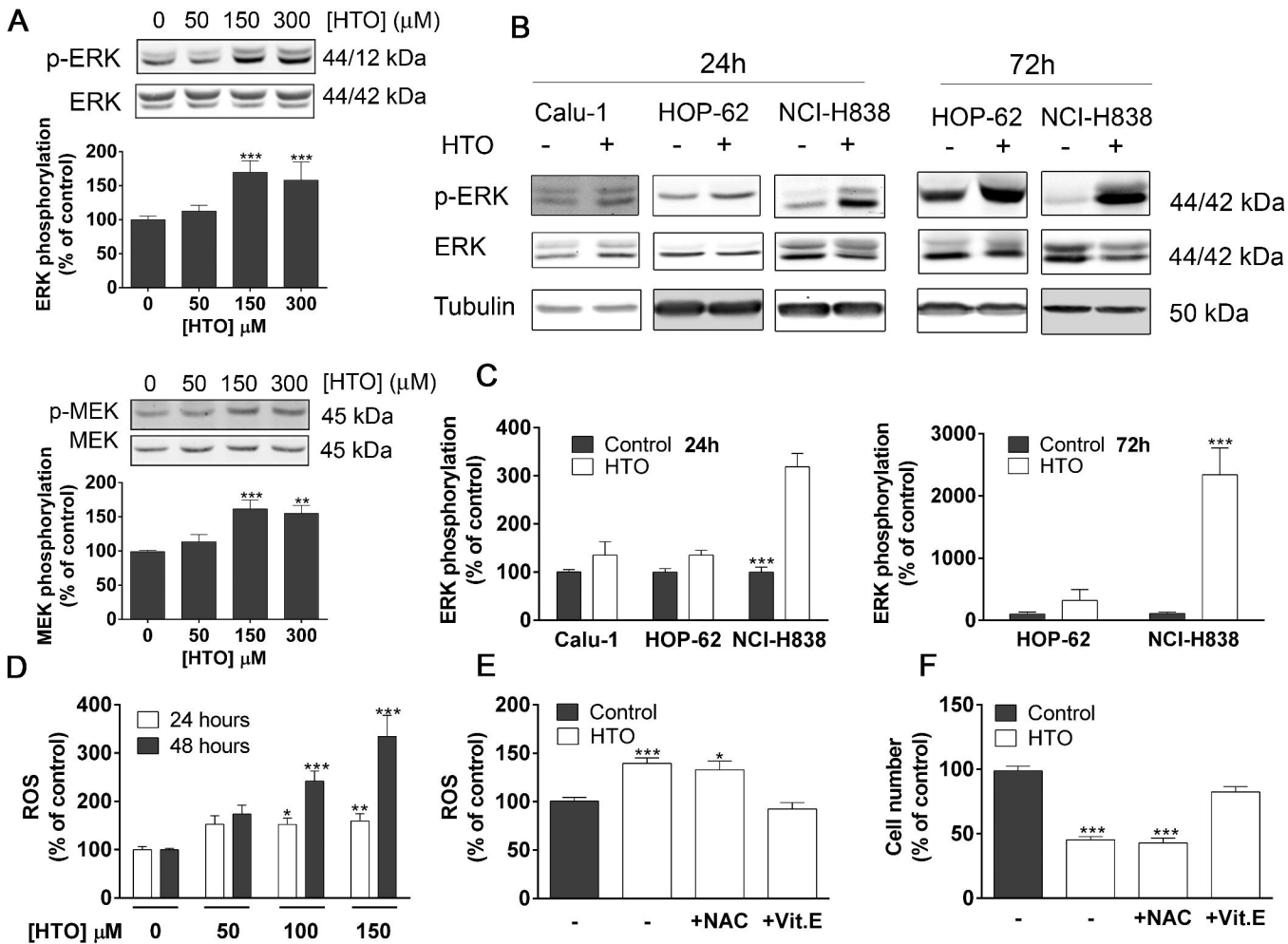
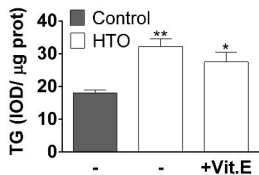
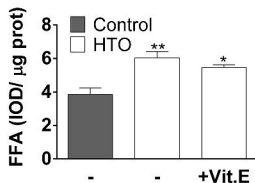
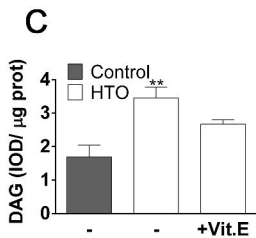
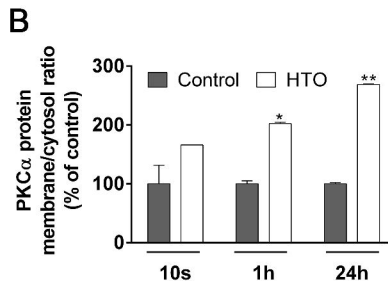
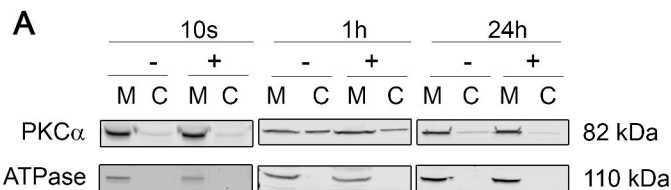


Fig. 2



**Fig. 3**



**Fig. 4**

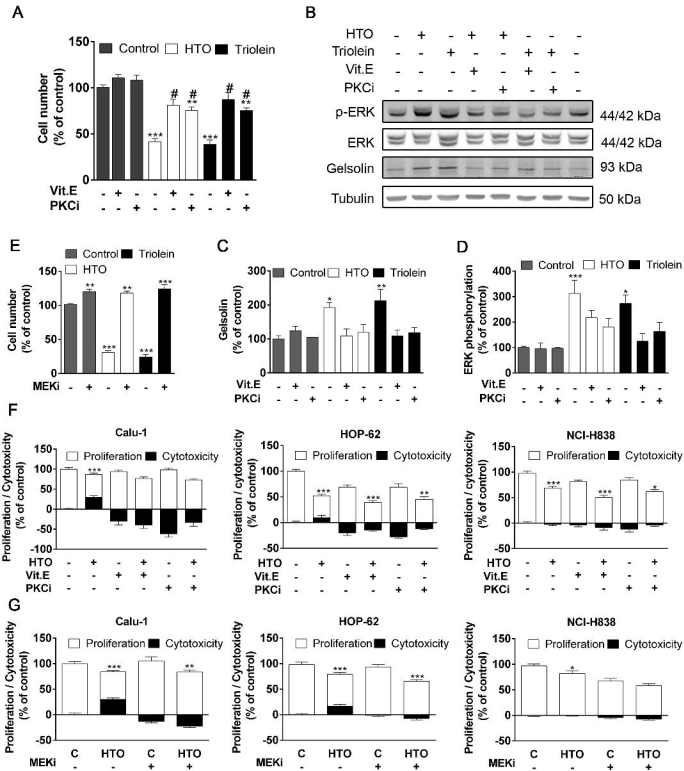
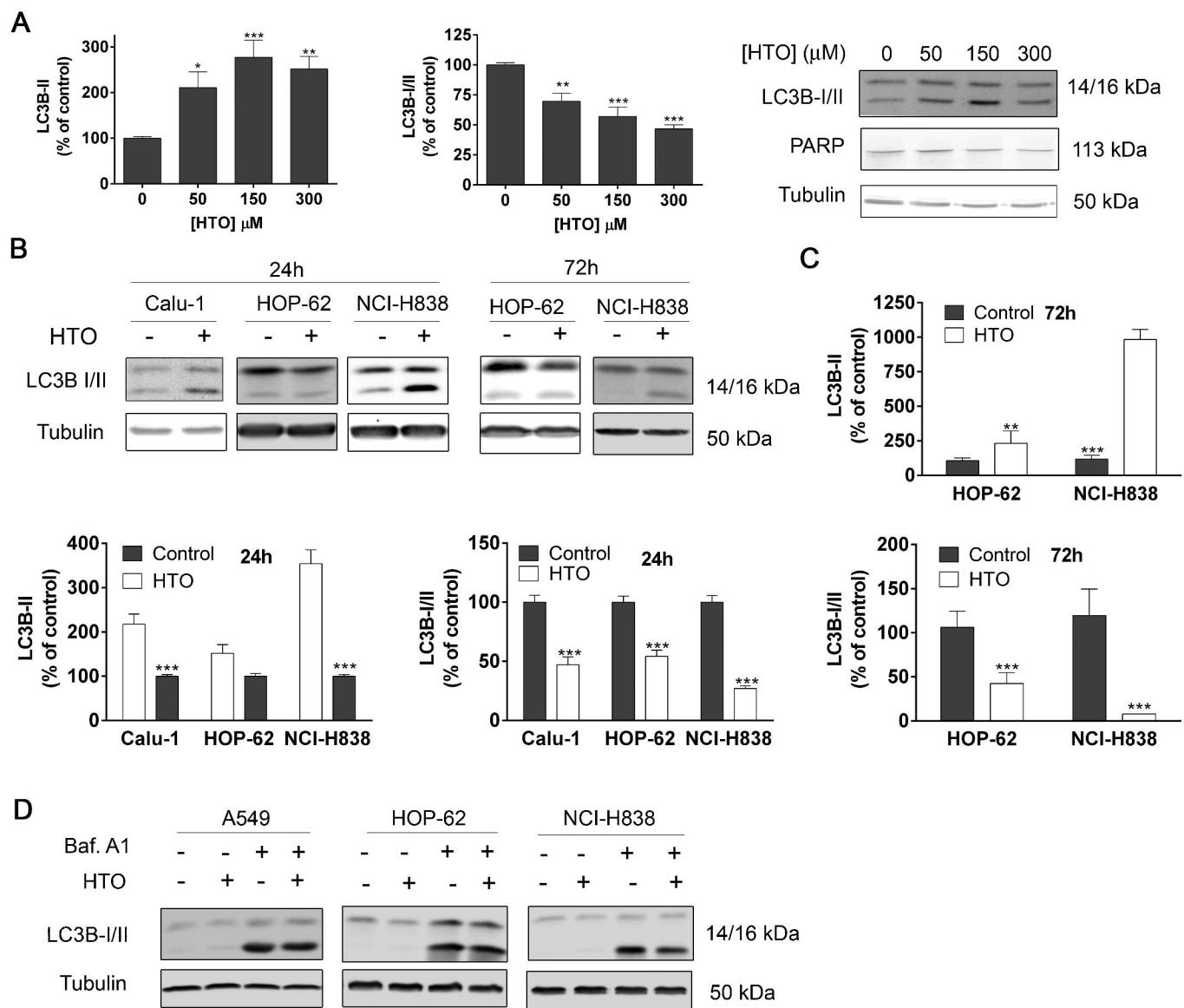
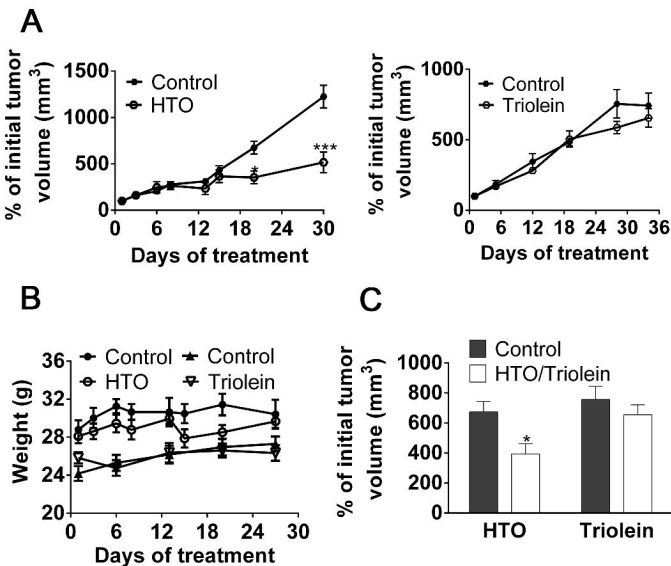


Fig. 5





**Fig. 6**



**Fig.7**

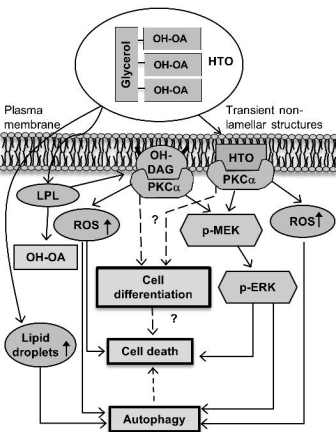


Fig. 8